International Journal for Multidisciplinary Research (IJFMR)
E-ISSN: 2582-2160 ● Website: www.ijfmr.com ● Email: editor@ijfmr.com

Structural and Morphological Study of Aluminium-doped M-type Barium Hexaferrite: $BaFe_{11.5}Al_{0.5}O_{19}$

Yaseen Mohd[1], Vijay Singh[2], Deepika Sharma[3]

[1]Center for Green Energy Research, Department of Physics, CPU, Hamirpur, Himachal Pradesh 176041, India
[2,3]Department of Physics, Himachal Pradesh University, Shimla, 171005, India

Abstract:
The structure of the material plays an important role in determining the electrical, magnetic, and electromagnetic properties of the material. Aluminium-doped M-type barium hexaferrite, $BaFe_{11.5}Al_{0.5}O_{19}$ has been prepared using the sol-gel auto-combustion method and systematically studied to understand the structural and morphological properties of the resultant materials. The formation of the crystalline phase of M-type hexaferrite with a hexagonal structure and space group P6 3/mmc was confirmed by X-ray diffraction (XRD) analysis, which was to be found in good agreement with standard XRD data. The detailed structural analysis was performed using Rietveld refinement, which led to the determination of lattice constants a = 5.881 Å, c = 23.17 Å, and V_{cell} = 694.076 $Å^3$. The refined occupancy shows that Al^{3+} ions mostly prefer 2a and 12k sites, and there is little occupancy at the bipyramidal site. The 2Θ angle and hkl planes calculated from the refined pattern are also in good agreement with the observed angle and planes of M-type barium hexaferrite. The morphological study of the ferrite has been done using FE-SEM. The images revealed crystalline particles with spherical and polyhedral shapes, and a few hexagonal grains were also observed.

Keywords: M-type ferrite, Structural study, Rietveld refinement, XRD analysis

1. Introduction

M-type hexaferrite has the general chemical formula $BaFe_{12}O_{19}$, have been utilized as a permanent magnet since its invention in the early 1950s. They have been used in these applications due to their superior chemical stability and suitable hard magnetic properties, like c-axis magnetic anisotropy, high coercivity, and excellent saturation magnetization (M_s) [1,2]. The improvement in magnetic properties is important because M-type hexaferrite has become an effective alternative to permanent magnets in many high-power applications. Various studies have shown how to improve the uniaxial magneto-crystalline anisotropy constant (K) and Ms of M-type hexaferrite by substituting different cations [2]. People have done various work to increase the magnetic properties of the M-type hexaferrite material. The value of M_s has increased in M-type hexaferrite with dopant elements La-Zn [3], Mn-Zn [4], and La-Ce [5]. The selective replacement of Fe^{3+} ions with spin orientations antiparallel to the net magnetisation direction by non-magnetic Zn^{2+} ions is one explanation for the rise in M_S. On the other hand, different elements have been studied to improve the coercivity (H_c) of the material. The H_c of the material has been improved via dopant

elements Mn^{3+} [6], Al-Pr [7], Al-Nd [8], Cr^{3+} [9], Al^{3+} [10] etc. To improve the magnetic and electromagnetic properties of any type of material, it is important to deeply analyse the structure of that material. Structural study of any material plays an important role in selecting the dopant and analysing the magnetic properties of ferrites. This study explores the deep structural analysis of aluminium-doped M-type hexaferrite, i.e. $BaFe_{11.5}Al_{0.5}O_{19}$.

The unit cell of M-type Ba-hexaferrite has 2 molecules in total, where one molecule contains 32 atoms; therefore, the unit cell contains 64 atoms. Br^{2+} and O^{2-} are both large and closely packed, where Fe^{3+} ions are located in interstices [11]. Here, the ions are coordinated in 1- tetrahedral 2 - FeO_4 ($4f_1$), 1 - Triangular bipyramidal 1-FeO_5 (2b), and 3 - octahedral 9- FeO_6 (2a, 12k, $4f_2$) sites. The structure is represented via alternate stacks of spinal and hexagonal layers, Fe_2O_2- and $bAFe_6O_2$. Here 24 Fe^{3+} ions arranged in 5 different sites are coupled by super exchange interaction via O^{2-}. The magnetic moment of SFO comes from Fe^{3+} ions, where one Fe^{3+} ions have magnetic moment of $5\mu_B$ [12]. Out of 12 Fe atoms, 8 are spin up, i.e., at 2a, 12k, and 2b sites, and 4 are spin down i.e. at $4f_2$ and $4f_1$, therefore, net magnetic moment is given as 4*5 = 20 μ_B [13].

2. Experimental Details

M-Type hexaferrite is synthesized using the sol-gel auto-combustion technique with different kinds of doping. Nano powders of ferrites are obtained from this method, which provides many advantages such as high powder purity, crystallinity, chemical homogeneity, and low equipment costs [14]. Extremely pure reagents include ferric nitrate nonahydrate $Fe(NO_3)_3.9H_2O$, barium nitrate $Ba(NO_3)_2$, Aluminium nitrate $Al(NO_3)_2$, citric acid anhydrous $C_6H_8O_7$, and ethylene glycol $C_2H_6O_2$.

Citric acid is a chelator, which forms complexes with metal ions and prevents hydroxyl-containing substances from precipitation. Since the salts serve as low-temperature NO3 oxidants that dissolve in water, they are used as initiators. Ethylene glycol acts as a surfactant, avoiding agglomeration and creating nanoparticles. As can be seen from Fig. 1, adding ethylene glycol to the solution at 80 °C enhances the exothermic effect and decreases the ignition temperature; thus, it makes possible the preparation of single-phase hexaferrite. Moreover, it can be used for controlling the viscosity of the solution and cation-cation exchange rate [15]. It takes 20-25 ml of pure water and constant stirring to completely dissolve the metal nitrates in a stoichiometric ratio, resulting in a transparent solution.

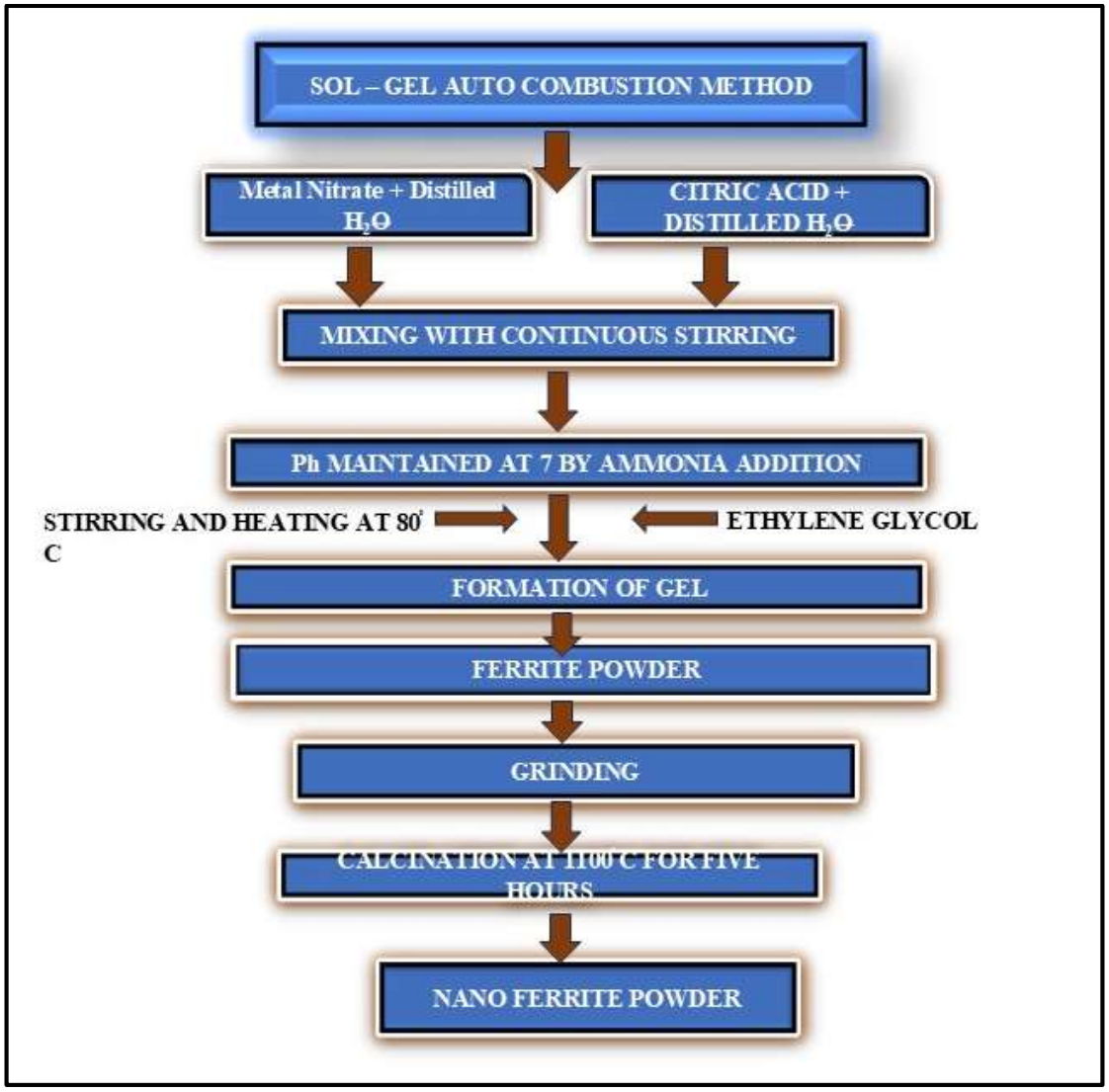

Figure 1: Pictorial representation of the sol-gel auto-combustion method for the preparation of Al-doped M-type barium hexaferrite.

3. Results and Discussion

3.1 XRD Rietveld refinement

Figure 2 displays the X-ray diffraction (XRD) patterns of $BaFe_{11.5}Al_{0.5}O_{19}$ at room temperature. These patterns showed that the produced magnetic nanoparticles are polycrystalline in nature.

The patterns reveal that a single-phase structure was successfully created for Al-doped M-type Ba hexaferrite, which is consistent with the standard JCPDS Card (International Centre for Diffraction Data (ICDD), powder diffraction file no. 00-33-1340)for M-type barium hexaferrite [16]. The strongest (114) reflection is visible in all patterns, and the M-type hexaferrite crystallizes in a hexagonal structure with space group $P6_3/mmc$.

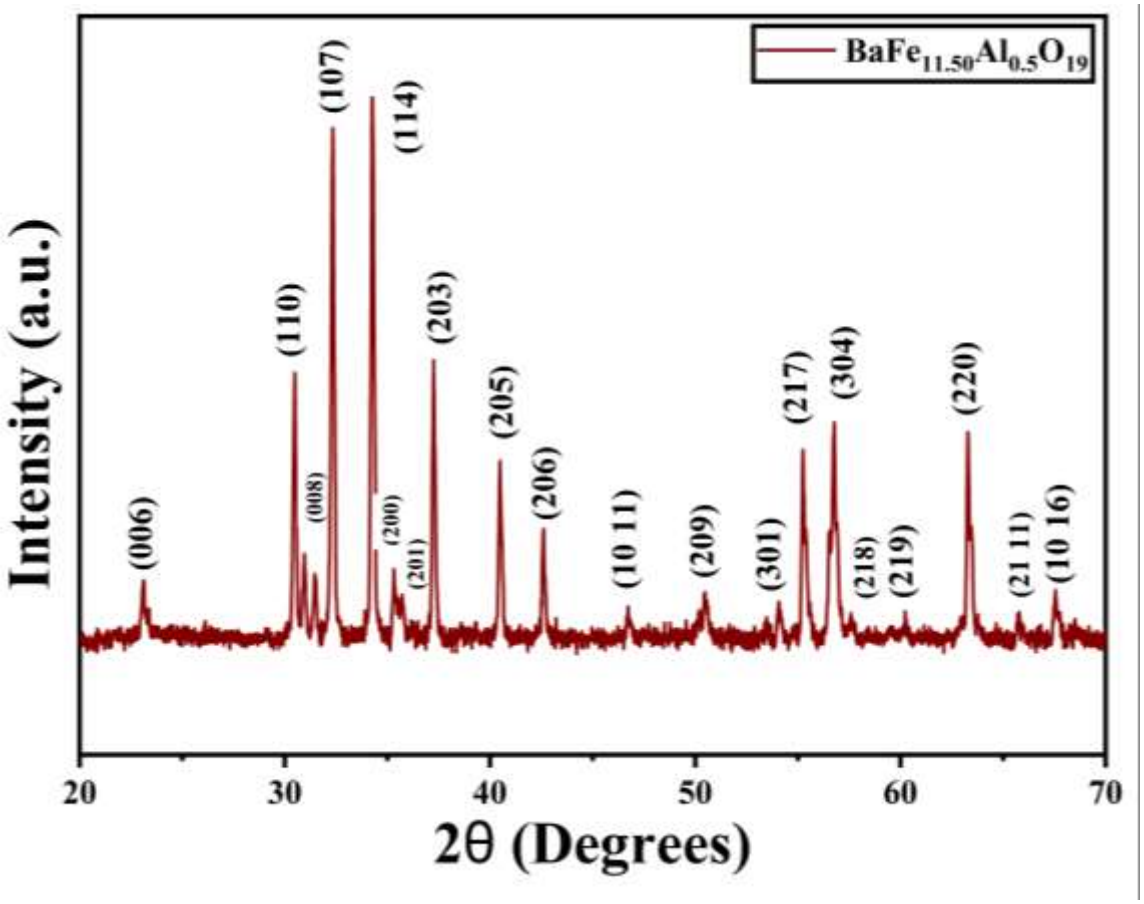

Figure 2: XRD Pattern for Al-doped M-type hexaferrite, $BaFe_{11.50}Al_{0.5}O_{19}$

Table 1: Structural Parameters for Al-doped M-type Ba-hexaferrite, $BaFe_{11.50}Al_{0.5}O_{19}$, obtained from Rietveld refinement pattern

a (Å)	5.881	R_p	19.9
c (Å)	23.17	R_{WP}	28.9
A (°)	90	R_e	3.82
γ (°)	120	X^2	2.41
V_{cell} ($Å^3$)	694.076	Density (g/cm^3)	5.436

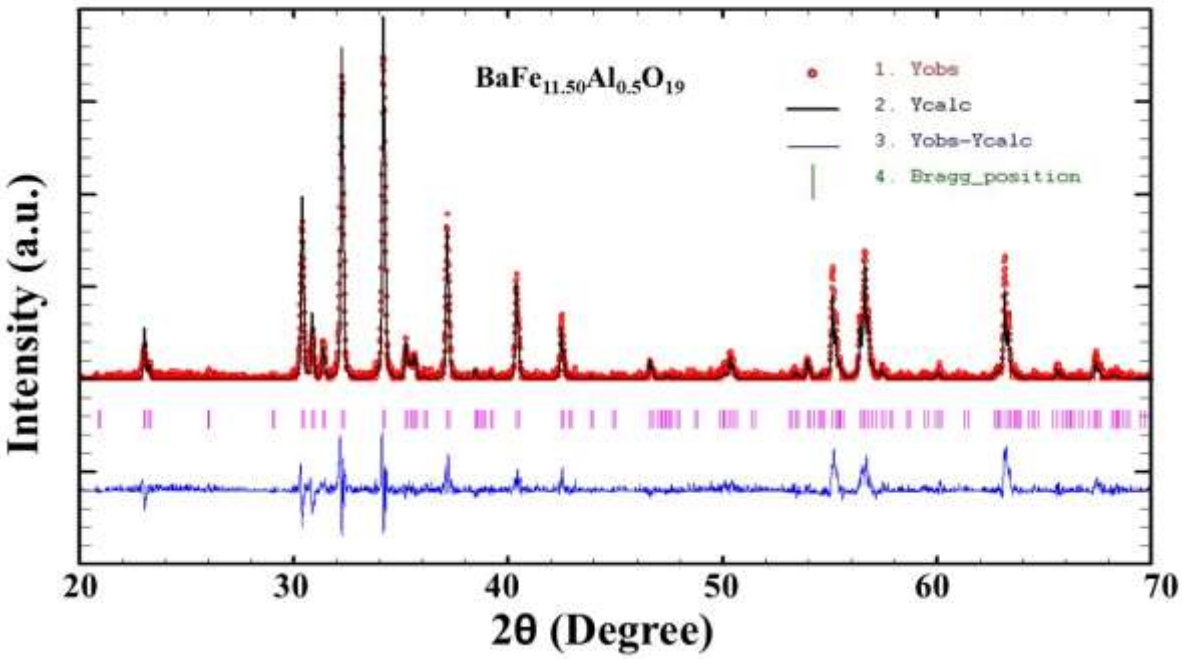

Figure 3: XRD Rietveld refinement for Al-doped M-type Ba-hexaferrite, $BaFe_{11.50}Al_{0.5}O_{19}$

It can be seen from Figure 2 that there are no signs of impurity peaks. The complete dissolution of aluminium into the M-type hexaferrite phase at 1100 °C is indicated by the absence of impurity peaks. The sample without impurity, i.e., the Fe_2O_3 phase, indicates the formation of a single M-type phase.
The Rietveld refinement method has been employed to conduct the deep phase analysis of the structure. Table 1 shows the values of different structural parameters. The values of lattice constants a (Å) and c (Å) are 5.881 and 23.17, respectively. The cell volume ($Å^3$), and density (g/cm^3) are 694.076 and 5.436, respectively. The values of other parameters used to define the fitting parameters, such as R_p, R_{wp}, R_e, and χ^2 are also shown in Table 1. R_{wp} is the weighted profile factor that denotes the degree of matching between the observed and calculated intensities. The statistically expected minimum value of R_{exp} (also named R_e) is based on the counting statistics, as well as the number of observations and refined parameters. The goodness of fit is expressed as :

$$GOF = \frac{R_{wp}}{R_{exp}}$$

Or in some programs:

$$\chi^2 = \left(\frac{R_{wp}}{R_{exp}}\right)^2$$

A GOF value close to 1 and a $\chi 2$ value close to 1 mean that the difference between the observed and expected values is near the expected statistical uncertainty. The high value of R_{wp} does not directly imply an incorrect structural model, but it can be due to background or peak-shape errors, preferred orientation, instrumental resolution, and counting statistics [17].

Table 2: The values of x, y, z, occupancy and multiplicity for Al-doped M-type Ba-hexaferrite, $BaFe_{11.50}Al_{0.5}O_{19}$

Atoms	Sites	x	y	z	Occupancy	Multiplicity
Ba_1	-	0.66670	0.33330	0.25	0.08107	2

Fe_1/Al_1	$(2a)_{oh}$	0.00	0.00	0.00	0.05751/0.0251	2
Fe_2/Al_2	$(12k)_{oh}$	0.00	0.00	0.25656	0.06235/0.0189	4
Fe_3/Al_3	$(4f)_{oh}$	0.3330	0.66670	0.02532	0.1632/0.0104	4
Fe_4/Al_4	$(4f)_{td}$	0.3330	0.66670	0.19260	0.1690/0.00103	4
Fe_5/Al_5	$(4e)_{bp}$	0.1686	0.33735	0.10827	0.4678/0.022	12
O_1	(4e)	0.00	0.00	0.15214	0.17006	4
O_2	(4f)	0.33330	0.66670	0.05799	0.18422	4
O_3	(6h)	0.177770	0.35539	0.25	0.27774	6
O_4	(12k)	0.16444	0.32887	0.05052	0.50136	12
O_5	(12k)	0.50038	0.00075	0.14557	0.45644	12

Table 3: The (hkl) values and 2Θ (º) angle obtained from XRD-Rietveld refinement for Al-doped M-type Ba-hexaferrite, $BaFe_{11.50}Al_{0.5}O_{19}$

(hkl)	**2Θ (º)**	**(hkl)**	**2Θ (º)**
110	30.37	10 11	46.620
008	30.845	209	50.357
107	32.225	300	53.964
114	34.167	217	55.146
201	35.432	304	56.432
203	37.143	20 11	56.661
116	38.545	220	63.189
205	40.380	20 14	67.428
206	42.485		

Table 2 shows the value of functional coordination in x, y, and z directions, occupancy, and multiplicity of 11 different sites of Al-doped M-type hexaferrite, i.e., $BaFe_{11.50}Al_{0.5}O_{19}$. The replacement of Al^{3+} has occurred at the site positions of Fe^{3+} ions. The site occupancy of Al^{3+} ions at different Fe sites has been clearly observed in Table 2. Al^{3+} preferentially occupies the spin-up octahedral $(2a)_{oh}$ site, octahedral (12 k) site, and bipyramidal $(4e)_{bp}$ site according to the refinement. At the spin-down site, the substitution is very minimal, as indicated by the refinement occupancy values given in Table 2. The results are in line with theoretical calculations by V. Dixit et al. [18], which show that $(2a)_{Oh}$ and $(12\ k)_{Oh}$ are the preferred substitution sites for Al. According to their estimates, the preference of the Al^{3+}ion occupying the $(4f)_{Oh}$, $(4f)_{Td}$, or $(4e)_{Bp}$ sites is substantially lower than that of the other two sites. The substitution of dopant ions at particular sites determines the magnetic, electrical, and electromagnetic properties of the material. According to Sharma et al [7], the substitution of diamagnetic Al^{3+} at spin-up sites is responsible for the decrease in saturation magnetization and remanence of the material.

The 2Θ position and corresponding (hkl) planes of the diffraction peaks identified for the M-type ferrite are summarized in Table 3. Both the high- and low-intensity diffraction peaks are shown in the table, which are resolved for the refined XRD pattern. The obtained values of 2Θ vs hkl are in good agreement with the reported values of the crystalline phase of M-type hexaferrite, confirming the formation of the desired crystalline phase.

3.2.Morphological study

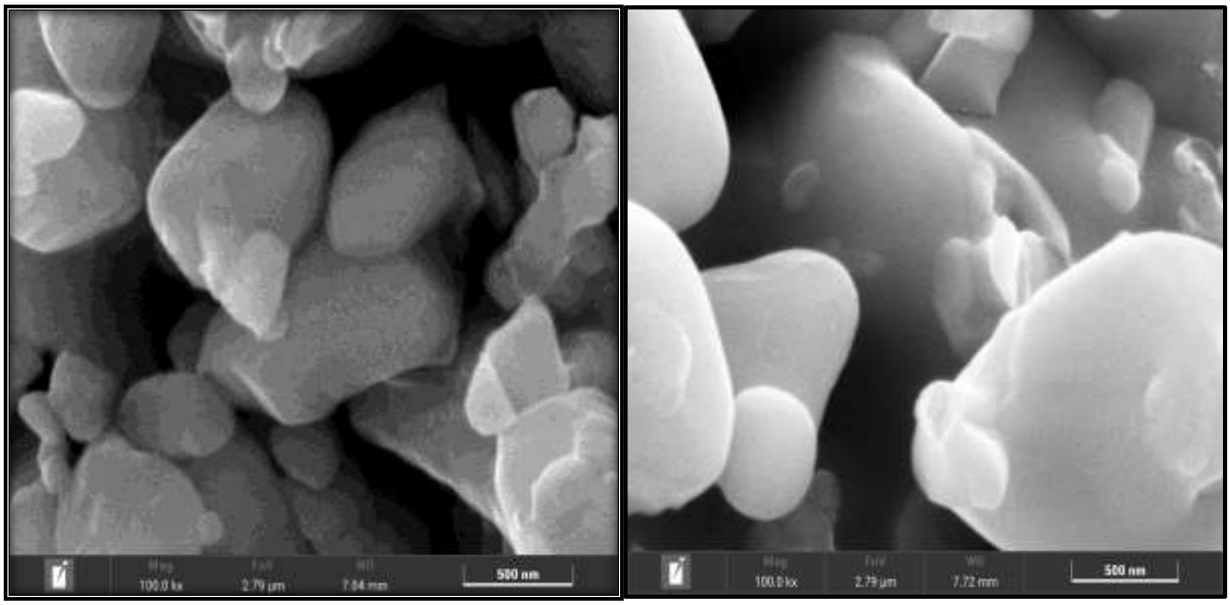

Figure 4: FESEM Micrographs at 500nm for Al-doped M-type Ba-hexaferrite, $BaFe_{11.50}Al_{0.5}O_{19}$

Figure 4 illustrates the FE-SEM micrographs at 500 nm for Al-doped M-type hexaferrite, $BaFe_{11.50}Al_{0.5}O_{19}$. All images were captured at 10,000× magnification using an In Lens detector. All compositions have a well-defined crystalline morphology, with a few particles appearing hexagonal in shape, accompanied by spherical and polyhedral grains. The overall shape of the BaM samples remains the same with Al substitution, while localized agglomerations occur due to magnetic interactions among the ions.

High porosity at the grain boundaries and more irregular grain morphology are observed due to aluminium substitution levels. Grain formation is inhibited by Al^{3+} ions, which have a smaller ionic radius than Fe^{3+} ions. They substitute into the Fe sites and impede grain boundary mobility. As a result, smaller but less dense microstructures with discernible intergranular holes are produced by Al incorporation. This microstructural evolution is expected to have a major effect on the material's magnetic anisotropy and dielectric response since grain size and porosity directly affect domain wall motion and interfacial polarization.

4. Conclusion :

The present work explores the structural and morphological study of Al-doped M-type Ba-hexaferrite, $BaFe_{11.5}Al_{0.5}O_{19}$, $BaFe_{11.5}Al_{0.5}O_{19}$ was synthesized successfully by using the sol-gel auto-combustion method and characterized by XRD, Rietveld refinement, and FESEM. The XRD analysis shows that the single-phase crystalline M-type hexagonal structure was successfully synthesized. The Rietveld refinement was done to have a detailed investigation of the structure. The values of lattice parameters, unit cell volume, density, functional co-ordinates in x, y and z direction, occupancy and multiplicity have been observed for $BaFe_{11.5}Al_{0.5}O_{19}$. These structural parameters help to determine the occupancy of dopant ions. These results will be helpful for the deep analysis of the electrical, magnetic, and electromagnetic properties of the material. The SE-SEM micro-graphs showed that the agglomeration of the particles due to the magnetic nature of the samples, grain boundary porosity, and well-defined crystalline morphology consists of spherical and polyhedral grains with a few hexagonal particles. The results of the overall study

gives the correlation between Al^{3+} substitution, crystal structure, site occupancy and microstructural evolution, which is useful for structural insights of Al doped M-type barium hexaferrite for permanent-magnet applications.

References:

1. R.C. Pullar, Hexagonal ferrites: A review of the synthesis, properties and applications of hexaferrite ceramics, Prog. Mater. Sci. 57 (2012) 1191–1334. https://doi.org/10.1016/J.PMATSCI.2012.04.001.
2. J.P. Lim, M.G. Kang, Y.M. Kang, Development of Multi-Cation-Doped M-Type Hexaferrite Permanent Magnets, Applied Sciences 2023, Vol. 13, 13 (2022). https://doi.org/10.3390/APP13010295.
3. S. Lu, Y. Liu, Q. Yin, J. Chen, J. Wu, J. Li, P. Zhang, Z.C. Chen, Investigation of crystal structure, Raman spectroscopy and magnetic properties of La-Zn substituted oriented M-type hexagonal barium ferrites, Mater. Res. Bull. 172 (2024) 112640. https://doi.org/10.1016/J.MATERRESBULL.2023.112640.
4. I. Ismail, M.M. Muhammad Zulkimi, R.S. Azis, M.S. Mustaffa, M.N. Hamidon, M. Ertugrul, Y.O. Yesilbag, F.N. Tuzluca, I. helina Hasan, G. Ozturk, U.C. Hasar, Effect of Mn and Zn doping on natural resonance frequency of strontium U-type hexaferrite and its performance as electromagnetic wave absorbers, J. Alloys Compd. 898 (2022) 163246. https://doi.org/10.1016/J.JALLCOM.2021.163246.
5. A. Azhar, M. Hussain, R. Akram, Z. Sarfraz, A. Iqbal, Microstructural and Magnetic Properties of La-Ce co-Doped Soft-Hard Ferrites Synthesized by the Co-precipitation Method, Journal of Superconductivity and Novel Magnetism 2025 38:5 38 (2025) 217-. https://doi.org/10.1007/S10948-025-07050-2.
6. F. Tenorio-González, … A.B.-M., Crystal structure and magnetic properties of high Mn-doped strontium hexaferrite, Journal of Alloys and Compounds 695 (2017) 2083–2090. https://doi.org/https://doi.org/10.1016/j.jallcom.2016.11.047.
7. D. Sharma, Rohit, V. Singh, A. Dogra, M. Singh, Aluminium and praseodymium doped M-type hexaferrites for electric vehicle applications, Ceram. Int. 50 (2024) 24815–24822. https://doi.org/10.1016/J.CERAMINT.2024.04.217.
8. D. Sharma, R. Duglet, V. Singh, Y. Mohd, A. Dogra, M. Singh, Tailoring magnetic parameters of M-type hexaferrites via Nd-Al doping for rare earth free permanent magnet in EV's, Phys. Lett. A 579 (2026) 131517. https://doi.org/10.1016/j.physleta.2026.131517.
9. S. Katlakunta, S. Meena, … S.S.-M.R., Improved magnetic properties of Cr3+ doped SrFe12O19 synthesized via microwave hydrothermal route, Mater. Res. Bull. 63 (2015) 58–66. https://doi.org/https://doi.org/10.1016/j.materresbull.2014.11.043.
10. H. Luo, B.K. Rai, S.R. Mishra, J.P. Liu, H. Luo, B.K. Rai, S.R. Mishra, V. V Nguyen, Physical and magnetic properties of highly aluminum doped strontium ferrite nanoparticles prepared by auto-combustion route, Journal of Magnetism and Magnetic Materials 324 (2013) 2602–2608. https://doi.org/10.1016/j.jmmm.2012.02.106.
11. M.R. Islam, M.K.R. Khan, M.S. Hossain, M.M. Rahman, M.M. Haque, M. Aliuzzaman, M.K. Alam, M.S.I. Sarker, Structural, thermodynamic, and magnetic properties of SrFe12O19 hexaferrite modified by co-substitution of Cu and Gd, RSC Adv. 14 (2024) 7314. https://doi.org/10.1039/d3ra08878b.
12. A. Verma, P. Pandeyb, P. Sharma, Strontium ferrite permanent magnet-An overview, Indian Journal of Engineering & Material s Sciences 7 (n.d.) 364–369.

13. A. Verma, O. Pandey, P. Sharma, Strontium ferrite permanent magnet-an overview, Indian Journal of Engineering and Materials Sciences (IJEMS 7 (2000) 364–369. http://nopr.niscpr.res.in/handle/123456789/24430 (accessed February 17, 2023).
14. A. Sutka, G. Mezinskis, Sol-gel auto-combustion synthesis of spinel-type ferrite nanomaterials, Front. Mater. Sci. 6 (2012) 128–141. https://doi.org/10.1007/S11706-012-0167-3.
15. A. Manhas, K.M. Batoo, M. Singh, Magnetic and Mössbauer investigations of soft Co2Z-type hexa nanoferrites, J. Alloys Compd. 767 (2018) 188–194. https://doi.org/10.1016/J.JALLCOM.2018.07.114.
16. J.P. Lim, M.G. Kang, Y.M. Kang, Development of Multi-Cation-Doped M-Type Hexaferrite Permanent Magnets, Applied Sciences 2023, Vol. 13, 13 (2022). https://doi.org/10.3390/APP13010295.
17. L.B. Mccusker, R.B. Von Dreele, D.E. Cox, D. Louër, P. Scardi, Rietveld refinement guidelines, Urn:Issn:0021-8898 32 (1999) 36–50. https://doi.org/10.1107/S0021889898009856.
18. V. Dixit, C.N. Nandadasa, S.G. Kim, S. Kim, J. Park, Y.K. Hong, L.S.I. Liyanage, A. Moitra, Site occupancy and magnetic properties of Al-substituted M-type strontium hexaferrite, J. Appl. Phys. 117 (2015). https://doi.org/10.1063/1.4922867/567917.